

Dynamical Motifs: Building Blocks of Complex Dynamics in Sparsely Connected Random Networks

Valentin P. Zhigulin

*Department of Physics, California Institute of Technology, Pasadena, California 91125, USA
and Institute for Nonlinear Science, University of California, San Diego, La Jolla, California 92093-0402, USA*
(Received 13 November 2003; published 8 June 2004)

Spatiotemporal network dynamics is an emergent property of many complex systems that remains poorly understood. We suggest a new approach to its study based on the analysis of **dynamical motifs**—small subnetworks with periodic and chaotic dynamics. We simulate randomly connected neural networks and, with increasing density of connections, observe the transition from **quiescence** to **periodic** and **chaotic dynamics**. This transition is explained by the appearance of dynamical motifs in the structure of these networks. We also observe domination of periodic dynamics in simulations of spatially distributed networks with local connectivity and explain it by the absence of chaotic and the presence of periodic motifs in their structure.

DOI: 10.1103/PhysRevLett.92.238701

PACS numbers: 89.75.Hc, 05.45.-a, 82.39.Rt, 87.18.Sn

Dynamics in networks underlie the functioning of many complex systems, such as the brain [1], cellular regulatory machinery [2], ecosystems [3], and many others. These systems exhibit a wide repertoire of dynamics, ranging from periodic oscillations in cell cycle and brain rhythms to chaos in food webs and chemical reactions. Recently, rapid advancements have been made in our understanding of **statistical properties** of natural and artificial networks (for reviews, see [4,5,6]) and of traffic dynamics [7] and transport processes [8,9] on them. However, still very little is understood about oscillatory dynamics in such networks.

The fundamental problem that one faces while trying to understand dynamics in complex networks is the strong influence of their structure on their non-Hamiltonian dynamics. This influence induces long term connectivity-dependent spatiotemporal correlations, which present a formidable problem for understanding the dynamics. Statistical methods allow us to solve this problem in the limit of infinite-size networks [10], but they are not applicable to the study of realistic networks with nonuniform connectivity and a relatively small size.

It was recently found that many real networks include statistically significant subnetworks, so-called **motifs**, in their structure [11]. In this Letter we suggest the use of **dynamical motifs**—small subnetworks with nontrivial dynamics—as a new approach to the study of oscillatory dynamics in complex networks. **In this approach we combine dynamical and statistical methods to identify dynamical motifs and to evaluate the probability of their occurrence in the structure of networks. We show that the emergence of periodic and chaotic dynamics in networks of increasing structural complexity is linked to the appearance of periodic and chaotic motifs in their connectivity.** We also consider spatially distributed networks with local connectivity and show that chaotic motifs are absent from their structure.

In many complex systems the dynamics of individual elements and the rules of their interaction are relatively simple, and the **resulting complex behavior is an emergent consequence of these interactions.** Hence, in order to study the influence of the structure on the dynamics of networks, **let us focus on models with simplest interactions and dynamics at each node.** Let $x_i(t) \in [0; 1]$, $i = 1, \dots, N$, be a set of variables describing properly scaled states of **N elements** connected in a network. Consider the time evolution of **network's state** vector $X(t) = \{x_1(t), x_2(t), \dots, x_N(t)\}$ described by the following set of first order differential equations:

$$\frac{dX(t)}{dt} = -X(t) + F[X(t)], \quad (1)$$

where $F(X) = \{f_1(X), f_2(X), \dots, f_N(X)\}$ is a set of **sigmoid nonlinearities with $[0; 1]$ value ranges.** This general class of models includes a continuous version of Random Boolean (Genetic) Networks (cRBN) [12,13], in which $f_i(X)$ are randomly chosen **Boolean** functions of their arguments, and continuous-time **Artificial Neural Networks** (cANN) [14], in which $f_i(X) = f[(\tilde{W} \cdot X)_i + \sigma_i]$, where \tilde{W} is the coupling matrix and σ_i are thresholds. Both of these models were shown to exhibit complex periodic and chaotic dynamics in the biologically relevant cases of intermediate probabilities of gene expression in cRBN [13] and nonsymmetric interactions in cANN [10].

To illustrate the use of dynamical motifs, we employ a simple **cANN** model with $f(x) = [1 + \exp(-20x)]^{-1}$, a uniform external excitation $\sigma_i = \sigma = 0.5$, and inhibitory interactions of the same strength: $\tilde{W} = -\tilde{G}_w$, where $w = 5$ and \tilde{G} is the adjacency matrix of the directed graph on which the network is defined. In this setting, the model is similar to the simplified version of a balanced network model [15], with excitatory connections replaced by a uniform field, and can be viewed as a simple

model of a cortical microcircuit. It is also an extension of the concept of winnerless competitive networks [16] to the case of random connectivity. However, methods presented in this Letter can be used for other models of the dynamics, such as Lotka-Volterra competition, etc.

We have performed **Monte Carlo simulations** of the above described cANN model defined on an ensemble of random networks with **$N = 200$ nodes and uniform probability p of node-to-node connections**, i.e., an **Erdős-Rényi (ER) ensemble**. A sample of $2 \times 10^4 p$ random networks was generated for each considered p and cANN dynamics was simulated 100 times on each of the networks, each time starting with a different initial condition taken at random from the hypercube $R_{(0,1)}^{200}$. Sets of initial conditions were considered in order to eliminate the influence of the basins of attraction in multistable networks, which in itself is a complicated issue requiring separate research. **The largest Lyapunov exponent λ was calculated in each simulation**. Networks with at least one initial condition leading to $\lambda \in (-0.005; 0.005)$, typically $\lambda \sim 10^{-4}$, were classified as **having limit cycle dynamics** and **with $\lambda > 0.005$, typically $\lambda \sim 10^{-1}$, as having chaotic dynamics**. As the probability of connections p was increased, the transition from fixed point to periodic and chaotic dynamics was observed around $p = 0.015$ (Fig. 1, triangles). The transition to **solely chaotic dynamics occurred around $p = 0.025$** (Fig. 1, squares).

Let us now apply the concept of dynamical motifs in order to explain these observations and make further predictions about oscillatory dynamics in networks. The main idea behind this **approach is that the transition to periodic or chaotic overall dynamics in a network occurs due to the appearance in its structure of small, not necessary isolated, dynamical motifs which have the same type of dynamics**. Of course, many of them may be present in a given dynamical network, but at least one is needed in order for the network to have a given type of

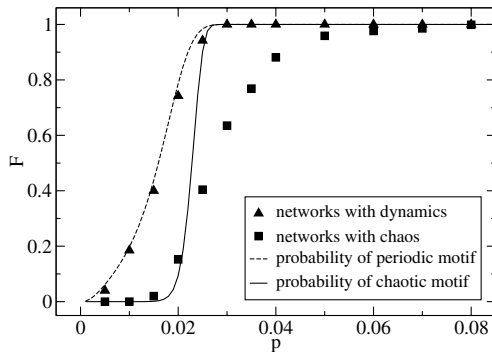


FIG. 1. Fraction of networks F with either periodic or chaotic (▲) and only chaotic (■) dynamics in simulations of 200-node cANN networks with node-to-node connection probability p . Lines represent predictions based on the probability of occurrence of periodic [dashed line, Eq. (5)] and chaotic [solid line, Eq. (6)] motifs.

dynamics. The dynamical phase transitions that are observed in models of complex networks are then identified with proliferation of dynamical motifs, i.e., 0-to-1 transitions in the probability of their occurrence.

Let us consider an **ER** network with the probability of node-to-node connection p . The probability p_n that some n nodes of this network form a given motif with l links and no self-loops is equal to $p^l(1-p)^{n(n-1)-l}$. It is possible that some of the nodes in the motif are suppressed by connections from a number f of nodes outside of a motif that are frozen in the “+1” state. Such inputs would suppress the dynamics of the motif and should be excluded. By doing so we obtain corrected probability

$$p_{nf} = p^l(1-p)^{n(n+f-1)-l}. \quad (2)$$

It is difficult to calculate exactly the probability to find $N_{(n;l)}$ such motifs in a network. However, approximate calculation of **the probability $P_{(n;l)}$ to encounter one or more motifs** is straight forward and is expected to work well in the case of sparsely connected networks ($p \ll 1$):

$$P_{(n;l)} = 1 - p(N_{(n;l)} = 0) \approx 1 - (1 - p_{nf})^{N!/A(N-n)!} \approx 1 - \exp\left(-\frac{p_{nf}N!}{A(N-n)!}\right), \quad (3)$$

where $N!/A(N-n)!$ is the number of ways to pick n nodes of the motif from the N -node network multiplied by $n!/A$ —number of ways to label a motif, with A being the order of motif’s automorphism group. This formula predicts proliferation of these motifs at some intermediate value of p , which depends on n and l . We are interested in the values of n and l for which proliferation occurs at the smallest $p = p_c$. Let us define it by the point where $P_{(n;l)} = 1/2$. Then

$$\frac{N!}{(N-n)!A} p_c^l (1-p_c)^{n(n+f-1)-l} = \log 2. \quad (4)$$

Assuming $N \gg n$ and $p_c \ll 1$, we find that $p_c \sim A^{1/l} N^{-n/l}$. To minimize p_c , n/l should be maximized and hence subnetworks with most nodes and least links will appear first as p is increased from 0.

Subnetworks with limit cycle dynamics include 3-loop [Fig. 2(a)], 4-loop, and other, more complicated structures. Since for the n -loop $l = n$ and $A = n$, 3-loop has smallest p_c . According to (3), its probability of occurrence is given by

$$P_{(3;3)} \approx 1 - \exp\left(-\frac{N^3}{3} p^3 (1-p)^{3(1+f)}\right) \quad (5)$$

and is plotted in Fig. 1 by a dashed line (with f evaluated numerically from simulations). This estimate predicts the appearance of dynamics in ER networks very accurately.

In order to find chaotic motifs we used the nauty package [17] to generate all possible nonisomorphic directed graphs with up to 8 nodes and 11 links, simulated the cANN dynamics on them, and calculated the largest

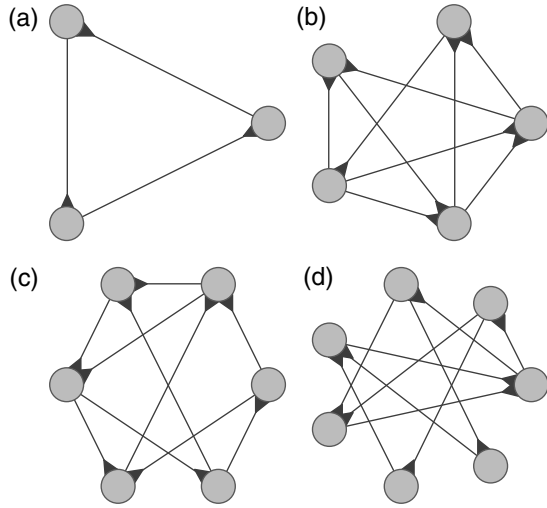


FIG. 2. Smallest dynamical motifs with periodic (a) and chaotic (b)–(d) dynamics. Small triangles indicate directions of the inhibitory connections.

Lyapunov exponent λ for each. Digraphs with $\lambda > 0.005$, typically $\lambda \sim 10^{-1}$, were classified as chaotic. In Figs. 2(b)–2(d) we show the first three chaotic motifs in the order of increasing number of nodes (five, six, and seven nodes) and minimal number of links (nine, ten, and ten links). Also, we found six nonisomorphic chaotic motifs with 8 nodes and 11 links, four of them with $A = 2$ and two with $A = 1$. Numerical evaluations of p_c according to (4) indicate that the latter motifs have smallest $p_c \approx 0.025$. Probability to find one or more of them in an ER network is given by

$$P_{(8;11)} \approx 1 - \exp[-4N^8 p^{11}(1-p)^{45+8f}] \quad (6)$$

and is plotted in Fig. 1 by a solid line (with f evaluated from simulations of chaotic networks). As can be seen from the plot, this prediction is reasonably good. The discrepancy may be caused by the approximate nature of the estimate (3), severe undersampling of the network space in simulations and disregard of the fact that not only frozen, but also periodically oscillating external nodes suppress chaos in these motifs.

While the origin of periodic dynamics in n -loops is obvious, as they merely are negative feedback loops, the nature of chaos in chaotic motifs is not self-evident. We have traced the route to chaos in the first chaotic motif by lowering w to 0.5 and then gradually increasing it. In Fig. 3 the bifurcation diagram of the local maxima of $x_1(t)$ oscillations is plotted. This diagram reveals two period doubling cascades, one starting around $w = 0.7$ and another one around $w = 2.5$.

However, there are no conclusive experimental observations of chaotic dynamics in either genetic or neuronal networks. Presence of chaotic dynamics would be inconsistent with the requirements of robustness and reproduc-

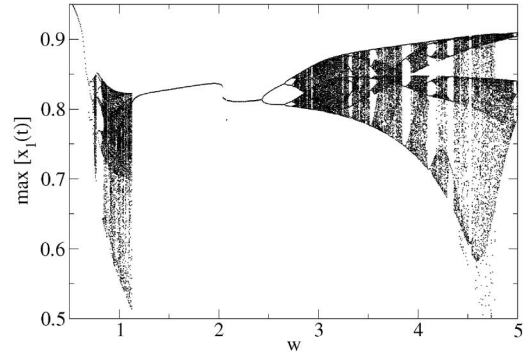


FIG. 3. Bifurcation diagram depicting local maxima of $x_1(t)$ oscillations for a range of strengths w of the inhibitory connections in the first chaotic motif [Fig. 1]. Period doubling cascades start around $w = 0.7$ and $w = 2.5$.

ibility of the response imposed on the living organisms by the environment. On the other hand, periodic dynamics in natural networks are very common. Hence, some of the assumptions that were used in the presented simplified model must be wrong. As we show below, one of them is the assumption of ER connectivity. Recent experimental data suggest that metabolic networks possess a scale-free structure [18], while neuronal networks are highly clustered on both short [19] and long [20] spatial scales. Moreover, neurons in the brain frequently form ordered spatial structures with distance-dependent probabilities of connections, so-called cortical microcircuits [21,22].

To illustrate the influence of spatial structure on the dynamical properties of networks, we simulated the cANN model on the 12×12 two-dimensional square lattice with neuron-to-neuron connection probabilities obeying Gaussian distribution and forbidden self-connections:

$$p(d_{ij}) = KN(1 - \delta_{ij})e^{-(d_{ij}/\gamma)^2} / \sum_{m,n=1}^N (1 - \delta_{mn})e^{-(d_{mn}/\gamma)^2}, \quad (7)$$

where d_{ij} is a metric distance between neurons i and j , γ is the length scale of the distribution, K is the average number of connections per neuron, and δ_{ij} is the Kronecker delta. In effect, γ controls clustering of the connectivity, with values close to 1 corresponding to networks with mostly local connectivity and large values effectively diminishing the role of spatial structure and corresponding to ER-like connectivity.

We generated a random sample of 1000 such networks with $\gamma = 2$ and $K = 14$. As in the case of an ER sample, cANN dynamics was simulated in each of the networks for 100 different random initial conditions and the largest Lyapunov exponent was calculated in each simulation. An average connectivity $K = 14$ corresponds to $p \approx 0.1$, which has led to approximately 99% of chaotic networks in a sample of ER ensemble [Fig. 1]. On the contrary,

around 99% of the networks with $\gamma = 2$ exhibited periodic dynamics and only about 1% were chaotic. This result indicates that clustering plays an important role in defining dynamical properties of neural networks and supports an observation that many real neuronal networks are locally clustered.

We now show how the idea of dynamical motifs may be used to understand these observations. Let us enumerate grid nodes by $1, \dots, N$ and consider a motif with n nodes and l links placed on the grid. We label its nodes by i_1, i_2, \dots, i_n and its links by $i_{a_1}i_{b_1}, i_{a_2}i_{b_2}, \dots, i_{a_l}i_{b_l}$ with $a_jb_j, j = 1, \dots, l$ denoting ordered pairs of nodes that are connected. Probability $P_{i_a i_b}$ for the grid nodes i_a and i_b to be connected is distance dependent and is given by (7). Then the average probability that n nodes of a network form this motif is obtained by averaging over all possible placements of its nodes on a grid:

$$p_n \approx \frac{1}{N^n} \sum_{i_1, \dots, i_n=1}^N \left(\prod_{j=1}^l P_{i_{a_j} i_{b_j}} \prod_{k=1}^s (1 - P_{i_{u_k} i_{v_k}}) \right), \quad (8)$$

where $s = n(n-1) - l$ and $u_k v_k$ are all the pairs of unconnected nodes. For example, an average probability for a 3-loop [Fig. 2(a)] is $p_3 = \frac{1}{N^3} \sum_{i_1, i_2, i_3=1}^N P_{i_1 i_2} P_{i_2 i_3} P_{i_3 i_1} (1 - P_{i_2 i_1}) (1 - P_{i_3 i_2}) (1 - P_{i_1 i_3})$. As expected, in the limit of distance-independent probabilities, expression (8) becomes equivalent to the ER case. Probability of occurrence of one or more motifs in a network can again be approximated by (3). It is approximately one for 3- and 4-loops and $P_{(5;9)} \approx 0$ for the (5;9) motif in networks with $\gamma = 2$. Other chaotic motifs would be even less probable because connection probability falls off quickly with distance in these networks. Also, $P_{(5;9)} \approx 1$ for the (5;9) motif in networks with $\gamma = 12$. Hence, periodic motifs are present and chaotic motifs are absent in spatial networks with local connectivity ($\gamma = 2$), but chaotic motifs are present in nonlocal networks with $\gamma = 12$. These calculations may also explain recent observations of periodic and chaotic dynamics in models of cortical neural microcircuits with local and nonlocal spatial organization of connectivity [22].

In conclusion, a method to study dynamical behavior of sparsely connected networks by examining minimal building blocks of the dynamics was suggested. **Calculation of the abundance of dynamical motifs in the structure of networks allows one to study and control dynamics in these networks by choosing connectivity that maximizes the probability of motifs with desirable dynamics and minimizes the probability of motifs with unacceptable dynamics.** Using this method we predict that connectivity of cortical networks might be such that it minimizes the occurrence of chaotic motifs in their structure.

In some real networks average node degree is high compared to $K \sim 10$ considered here. However, many of the connections are weak and were excluded from the

model, as they play minor role in the dynamics. **Hence, only the number of strong connections should be compared.** In the brain, for example, although a given neuron may be receiving on the order of 10^3 inputs, typically only about ten of them are strong.

It was shown in [11] that many real networks have 3-loops in their structure. In most cases there are very few of such loops, and it was argued that their presence is not statistically significant. However, we suggest that such dynamical motifs are important because the presence of even one or two of them may profoundly influence dynamical behavior of the whole network by slaving dynamics of many adjacent nodes.

The author would like to thank Ramon Huerta, Mikhail Rabinovich, Michael Cross, and Dmitri Chklovskii for useful discussions, Brendan McKay for extending his nauty package with digraphs, and Gilles Laurent for continuous inspiration and support. This work was partially supported by NSF Grants No. EIA-0130708 and No. EIA-0130746 and DOE Grant No. DE-FG03-96ER14592.

-
- [1] C. Koch and G. Laurent, *Science* **284**, 96 (1999).
 - [2] A. Goldbeter, *Nature (London)* **420**, 238 (2002).
 - [3] M. Kondoh, *Science* **299**, 1388 (2003).
 - [4] R. Albert and A. L. Barabasi, *Rev. Mod. Phys.* **74**, 47 (2002).
 - [5] S. N. Dorogovtsev and J. F. F. Mendes, *Adv. Phys.* **51**, 1079 (2002).
 - [6] M. E. J. Newman, *SIAM Rev.* **45**, 167 (2003).
 - [7] B. Tadic, S. Thurner, and G. J. Rodgers, *cond-man/0401094*.
 - [8] B. Tadic and S. Thurner, *Physica (Amsterdam)* **332A**, 566 (2004).
 - [9] I. Simonsen, K. A. Eriksen, S. Maslov, and K. Sneppen, *cond-mat/0312476*.
 - [10] H. Sompolinsky, A. Crisanti, and H. J. Sommers, *Phys. Rev. Lett.* **61**, 259 (1988).
 - [11] R. Milo *et al.*, *Science* **298**, 824 (2002).
 - [12] T. Mestl, R. J. Bagley, and L. Glass, *Phys. Rev. Lett.* **79**, 653 (1997).
 - [13] L. Glass and C. Hill, *Europhys. Lett.* **41**, 599 (1998).
 - [14] J. J. Hopfield, *Proc. Natl. Acad. Sci. U.S.A.* **81**, 3088 (1984).
 - [15] C. vanVreeswijk and H. Sompolinsky, *Science* **274**, 1724 (1996).
 - [16] M. I. Rabinovich *et al.*, *Phys. Rev. Lett.* **87**, 068102 (2001).
 - [17] B. D. McKay, *J. Algorithms* **26**, 306 (1998).
 - [18] H. Jeong *et al.*, *Nature (London)* **407**, 651 (2000).
 - [19] O. Shefi *et al.*, *Phys. Rev. E* **66**, 021905 (2002).
 - [20] C. C. Hilgetag *et al.*, *Philos. Trans. R. Soc. London B* **355**, 91 (2000).
 - [21] G. Silberberg, A. Gupta, and H. Markram, *Trends Neurosci.* **25**, 227 (2002).
 - [22] W. Maass, T. Natschlager, and H. Markram, *Neural Comput.* **14**, 2531 (2002).